ELSEVIER

Neurobiology of Disease

www.elsevier.com/locate/ynbdi
Neurobiology of Disease 31 (2008) 33–40

TLR-4 deficiency protects against focal cerebral ischemia and axotomy-induced neurodegeneration

Ulkan Kilic,[a,b] Ertugrul Kilic,[a,c,*] Christian M. Matter,[b] Claudio L. Bassetti,[a] and Dirk M. Hermann[a,d]

[a]*Department of Neurology, University Hospital Zürich, Frauenklinikstr. 26, CH-8091 Zürich, Switzerland*
[b]*Cardiovascular Research, Institute of Physiology, University Hospital Zürich, Winthertürerstrasse 190, CH-8057 Zurich, Switzerland*
[c]*Department of Physiology, Faculty of Medicine, Yeditepe University, TR-34755 Kayisdagı, Istanbul, Turkey*
[d]*Department of Neurology, University Hospital Essen, Hufelandstr. 55, D-45122 Essen, Germany*

Received 27 September 2007; revised 29 February 2008; accepted 13 March 2008
Available online 28 March 2008

The pattern recognition receptor toll-like receptor (TLR)-4 mediates innate danger signaling in the brain, being activated in response to lipopolysaccharide. Until now, its role in the degenerating brain remained unknown. We here examined effects of a loss-of-function mutation of TLR-4 in mice submitted to transient focal cerebral ischemia and retinal ganglion cell (RGC) axotomy, which are highly reproducible and clinically relevant *in vivo* models of acute and subacute neuronal degeneration. We show that TLR-4 deficiency protects mice against ischemia and axotomy-induced RGC degeneration. Decreased phosphorylation levels of the mitogen-activated kinases ERK-1/-2, JNK-1/-2 and p38 together with reduced inducible NO synthase levels in injured neurons of TLR-4 mutant mice suggests that TLR-4 deficiency downscales parenchymal stress responses, thereby enhancing neuronal survival. At the same time, densities of MPO+ neutrophils and Iba1+ microglial cells were increased in the brains of TLR-4 mutant animals, pointing towards a futile inflammatory response aiming to compensate lost functions. Our data indicate that innate immunity may represent an attractive target for neuroprotective treatments in stroke and neurodegeneration.

Keywords: Innate immune system; Danger signaling; Ischemic stroke; Neurodegeneration

The injured brain is particularly vulnerable to environmental stimuli. As such, brain cells may remain viable under conditions of ischemia or trauma, but activate death programs when exposed to additional stressors, such as organic toxins (Hermann et al., 2006) or pro-inflammatory signals (Bermpohl et al., 2005). To protect itself from injury, the brain has developed its own endogenous strategies.

Along the blood-brain barrier (BBB), so-called ATP-binding cassette (ABC) transporters are expressed on capillary cells that actively eliminate natural compounds from the brain (Begley, 2004; Löscher and Potschka, 2005; Hermann, and Bassetti, 2007). ABC transporters are specifically regulated in response to ischemia (Spudich et al., 2006) and other kinds of brain injury (Hermann et al., 2006; Hermann, and Bassetti, 2007), thus providing a highly efficacious barrier for environmental toxins.

In the surrounding of brain capillaries, perivascular dendritic and macrophages are located, which together with brain-resident microglia represent an innate surveillance system in the immune-privileged brain (Bechmann et al., 2007). This task is achieved by so-called pathogen-recognition receptors (PRR), which recognize conserved microbial motifs (Sansonetti, 2006; Sutmuller et al., 2006; Lee and Kim, 2007).

Among the pathogen-associated molecular patterns (PAMP) recognized by brain-resident microglia, lipopolysaccharides (LPS), i.e., cell wall constituents of gram-negative bacteria, play a very important role, being detected by a PRR termed toll-like receptor (TLR)-4 (Chakravarty and Herkenham, 2005). TLR-4 is a leucine-rich transmembrane protein, named after the toll protein in *Drosophila*, where this receptor family was first described (Lemaitre et al., 1996).

Once stimulated by LPS, TLR-4 activates a variety of signal pathways in the cytosol of immune cells. Via its cytosolic Toll/interleukin-1 (IL-1) receptor homology domain (TIR), TLR-4 stimulates mitogen-activated protein (MAP) and stress kinases, such as extracellular-regulated kinase (ERK)-1/-2, Jun kinase (JNK)-1/-2 and p38, which in turn activate transcription regulators of inflammation in the nucleus (Schröder et al., 2001). Activation of TLR-4 enables microglial cells to remove LPS from the brain tissue (Sutmuller et al., 2006).

In view of the complex downstream responses activated by LPS we wondered how TLR-4 deactivation influences cell injury under conditions in which neurons are lost. We therefore investigated the

* Corresponding author. Department of Neurology, University Hospital Zürich, Frauenklinikstr. 26, CH-8091 Zürich, Switzerland. Fax: +41 44 255 4507.
E-mail address: kilic44@yahoo.com (E. Kilic).
Available online on ScienceDirect (www.sciencedirect.com).

0969-9961/$ - see front matter © 2008 Elsevier Inc. All rights reserved.
doi:10.1016/j.nbd.2008.03.002

effect of the loss-of-function mutation of TLR-4 in the C3H/HeJ mouse line on injury development and cell signaling in two models of brain disease, i.e., i.) after focal cerebral ischemia, induced by intraluminal middle cerebral artery (MCA) occlusion (Kilic et al., 2006a; Bechmann et al., 2007), and ii.) after retinal ganglion cell (RGC) axotomy, induced by optic nerve (ON) transsection (Kilic et al., 2005a,b, 2006b).

Materials and methods

Animals

All experimental procedures were carried out with government approval according to NIH guidelines for the care and use of laboratory animals. Adult male C3H/HeJ mice, which carry a point mutation in the cytosolic domain of the TLR-4 protein resulting in the exchange of amino acid 712 from proline to histidine that abrogate receptor functionality (Poltorak et al., 1998), and TLR-4-wildype (wt) C3H/HeN controls were purchased from the Jackson Laboratory. Animals were subjected to transient focal cerebral ischemia, induced by 90 min or 30 min of MCA occlusion, or underwent RGC axotomy by ON transsection ($n=6$ animals/group).

Experimental procedures: Transient focal brain ischemia

Animals (9–11 weeks) were anesthetized with 1% halothane (30% O_2, remainder N_2O). Rectal temperature was maintained between 36.5 and 37.0 °C using a feedback-controlled heating system. During the experiments, blood flow was measured by laser Doppler flow (LDF) measurements using a flexible 0.5 mm fiber optic probe (Perimed, Stockholm, Sweden), which was attached to the intact skull overlying the middle cerebral artery (MCA) territory (2 mm posterior/6 mm lateral from bregma). LDF changes were monitored up to 30 min after the onset of reperfusion. Focal ischemia was induced using an intraluminal filament technique (Wang et al., 2005; Kilic et al., 2006a). A midline neck incision was made, and the left common and external carotid arteries were isolated and ligated. A microvascular clip (FE691, Aesculap, Tuttlingen, Germany) was temporarily placed on the internal carotid artery. A 8-0 nylon monofilament (Ethilon; Ethicon, Norderstedt, Germany) coated with silicon resin (Xantopren, Bayer Dental, Osaka, Japan; diameter of the coated thread: 190–200 μm) was introduced through a small incision into the common carotid artery and advanced 9 mm distal to the carotid bifurcation for MCA occlusion. Either 30 min or 90 min after MCA occlusion, reperfusion was initiated by withdrawal of the monofilament. Anesthesia was discontinued and animals were placed back into their cages. Twenty-four hours (90 min MCA occlusion) or 72 h (30 min) later, animals were deeply re-anesthetized and decapitated. Brains were removed and cut on a cryostat in 18 μm coronal sections.

Experimental procedures: Optic nerve (ON) transsection

For retrograde labeling of RGC, animals (12–14 weeks) were *i.p.* anesthetized with 7% chloral hydrate. The superior colliculi were exposed via a bur hole that was drilled into the pericranium 0.7 mm lateral to the sagittal suture and 3 mm posterior to the bregma. A Hamilton syringe was inserted 2.0 mm beneath the brain surface, and 0.7 μl of fluorogold (infusion rate 0.7 μl/min) was injected stereotactically into both superior colliculi (Kilic et al., 2005a,b, 2006b). After infusion, the injection needle remained inside the tissue for 2 min to prevent fluorogold diffusion along the needle track, before the syringe was withdrawn.

Four days after labeling, mice were re-anesthetized with 7% chloral hydrate. After skin incision close to the superior orbital rim, the right orbita was opened, leaving the supraorbital vein intact, and the lacrimal gland was resected subtotally. After spreading the superior extraocular muscles, the right ON was transected under microscopical control approximately 0.5 mm distant to the posterior pole of the eye, taking care not to damage the retinal blood vessels. The wounds were sutured and the retinal blood supply was verified by fundoscopy (Kilic et al., 2006b).

Fourteen days after ON transsection, mice were killed with an overdose of chloral hydrate and both eyes were removed. The retinas were dissected, flat-mounted on glass slides, and fixed in 4% paraformaldehyde (PFA) in 0.1 M phosphate-buffered saline (PBS) for 30 min.

Analysis of histological injury

Infarct volumetry and brain edema

Brain sections were fixed for 10 min with 4% PFA in 0.1 M PBS and subsequently stained with cresyl violet. For infarct volumetry and assessment of brain edema, a total of four sections from equidistant brain levels, 2 mm apart, were analyzed in animals submitted to 90 min MCA occlusion (sections selected starting from the rostral pole of the striatum: bregma +2.0 mm, subsequent sections taken from bregma 0.0, −2.0 and −4.0 mm). On these sections, brain infarcts were outlined by delineating non-lesioned tissue in both hemispheres, from which edema-corrected infarct areas and infarct volumes were calculated. Brain edema was analyzed by outlining lesioned and non-lesioned tissue in both hemispheres, which were subtracted from each other and divided by the non-lesioned tissue in the contralateral brain, thus calculating percentage values of brain swelling.

Analysis of surviving neurons

In animals submitted to 30 min MCA occlusion cresyl violet-stained sections from the bregma level were microscopically evaluated by counting the density of surviving medium-to-large-sized neurons in the striatum in a total of nine random regions of interest (ROI), 1 mm apart, each measuring 62,500 μm^2 (Wang et al., 2005). Stereological analysis was done by one of the investigators blinded for the experimental condition (Ü.K.). Mean values were calculated for all areas both ipsilateral and contralateral to the stroke. Thereby, the percentage of surviving neurons was determined.

Analysis of DNA-fragmented cells

From animals subjected to 30 min MCA occlusion, sections from the level of the mid-striatum (bregma 0.0 mm) were stained by terminal transferase biotinylated-dUTP nick end labeling (TUNEL) using a commercially available kit (Roche, Basle, Switzerland) (Kilic et al., 2006a). In these sections, DNA-fragmented cells were counted in blinded manner (again done by Ü.K.) in the same nine random ROI in the striatum (each 62,500 μm^2) as above.

Evaluation of RGC survival by stereology of surviving RGCs

Surviving RGCs were evaluated by fluorescence microscopy using retinal whole-mounts using a rhodamine filter (546/590 nm). RGC densities were determined by counting tracer-labeled RGCs in 12 random ROI (three areas per retinal quadrant at different eccentricities of 1/6, 3/6 and 5/6 of the retinal radius, respectively; measuring 62,500 μm^2 each) (Kilic et al., 2006b). Mean values were calculated for all eccentricities as well as over the whole retina.

Activation of MAP kinases ERK-1/-2, JNK-1/-2 and p38

Tissue samples harvested from the ischemic MCA territory of C3H/HeJ and C3H/HeN mice subjected to 30 min MCA occlusion (72 h reperfusion) were complemented with lysis buffer, homogenized and centrifuged. Supernatants were used for sodium dodecylsulphate-polyacrylamide gel electrophoresis (SDS-PAGE). Prior to processing, samples from animals belonging to the same experimental group ($n=6$ animals/group) were pooled. After SDS-PAGE, proteins were transferred onto PVDF membranes. Membranes were dried, incubated in blocking solution and immersed with polyclonal rabbit anti-total (=detecting both the phosphorylated and unphosphorylated forms) ERK-1/-2 (9102; Cell Signaling, Allschwil, Switzerland), mouse anti-phospho-ERK-1/-2 (M8159; Sigma, Deisenhofen, Germany), rabbit anti-total JNK-1/-2 (JNK-2, sc-572; Santa Cruz), rabbit anti-phospho-JNK-1/-2 (9251; Cell Signaling), rabbit anti-total p38 (9212, Cell Signaling) or rabbit anti-phospho-p38 (9211, Cell Signaling) antibody, each diluted 1:500 in 0.1% Tween 20/0.1 M Tris buffered saline (TBS) (Kilic et al., 2006b). Membranes were rinsed, incubated in peroxidase-coupled secondary antibodies, diluted 1:2000 in 0.1% Tween 20/0.1 M TBS, washed, immersed in enhanced chemoluminescence (ECL) solution and exposed to ECL-Hyperfilm (Amersham, Braunschweig, Germany). Protein loading was controlled with a monoclonal mouse antibody against anti-β-actin (A5316; Sigma). Blots were performed at least three times. Protein levels were analyzed densitometrically, corrected with values determined on anti-β-actin blots and expressed as relative values compared with wt mice.

Expression of activated caspase-3 and inducible NO synthase (iNOS)

Brain sections were fixed in 4% PFA in 0.1 M PBS, washed and immersed for 1 h in 0.1 M PBS containing 0.3% Triton X-100 (PBS-T)/10% normal goat serum. Sections were incubated overnight at 4 °C with polyclonal rabbit anti-activated caspase-3 (CM-1; BD Biosciences, Basle, Switzerland) or anti-iNOS (NOS-2, sc-650; Santa Cruz, Nunningen, Switzerland) antibody, diluted 1:100 in PBS-T. Counterstainings were performed with a monoclonal mouse antibody against the neuronal nuclear protein NeuN (MAB377; Chemicon, Lucerne, Switzerland; 1:500). After staining with Cy3-labeled (iNOS, caspase-3) and FITC-labeled (NeuN) secondary antibody, sections were incubated with 4′,6-diaminido-2-phenylidole (DAPI) and coverslipped. Sections were microscopically analyzed by counting activated caspase-3(+) and iNOS(+) cells in six random ROI each in the ischemic parietal cortex and ischemic striatum (62,500 μm^2), for which mean values were calculated (Kilic et al., 2006a).

Analysis of polymorphonuclear neutrophil (PMN) recruitment and microglial activation

For assessment of PMN recruitment, myeloperoxidase (MPO) stainings were prepared with Histostain®-*Plus* kits (Zymed Laboratories, San Francisco, CA). Microglial activation was evaluated by immunohistochemistry for ionized calcium binding adaptor protein-1 (Iba1). Brain sections were fixed in 4% PFA in 0.1 M PBS, washed in water and boiled in 0.01 M citrate buffer for 15 min for epitope retrieval. Sections were incubated in 0.3% H_2O_2 peroxidase quenching solution for 10 min, followed by serum blocking solution for 30 min. Sections were then incubated with rabbit anti-MPO (Zymed Laboratories, San Francisco, CA) and ant-Iba1 (Wako Chemicals GmbH, Neuss, Germany) antibodies, diluted 1:100 in 5% normal goat serum in 0.3% Triton X-100/0.1 M PBS for 60 min, followed by incubation in a biotinylated secondary antibody for 10 min. Following signal detection with diaminobenzidine, sections were counterstained with hematoxyline. MPO(+) PMN and Iba1(+) microglia were microscopically identified based on morphological criteria. PMNs were distinguished from eosinophilic and basophilic cells based on hematoxyline staining properties. Sections were analyzed by counting MPO(+) and Iba1(+) cells in six random ROI each in the ischemic parietal cortex and ischemic striatum (measuring 62,500 μm^2), for which mean values were calculated.

Statistics

All values are given as mean±SD. Differences between groups were compared by independent two-tailed *t*-tests. p values <0.05 were considered to indicate statistical significance.

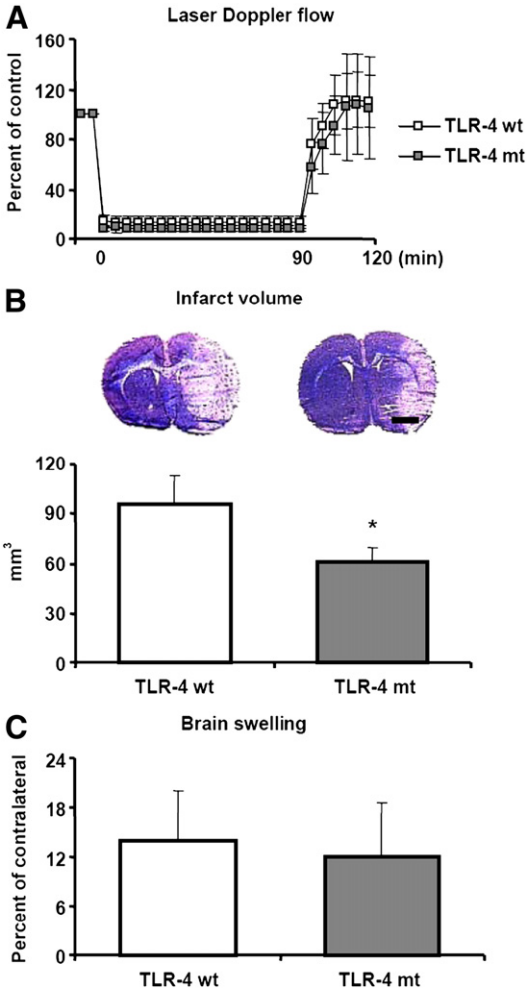

Fig. 1. TLR-4 deficiency reduces ischemic infarct volume after transient focal cerebral ischemia. Laser Doppler flow (LDF) during and after ischemia (A), infarct volume (B), and brain swelling (C) in TLR-4 wt and TLR-4 mt mice submitted to 90 min MCA occlusion, followed by 24 h reperfusion. Representative cresyl violet-stained sections are also shown (B). Note that LDF (A) and brain edema (C) do not differ between mouse lines. Data are means±SD ($n=6$ animals/mouse line). *$p<0.05$ (two-tailed *t*-tests). Bar, 2 mm.

Results

TLR-4 deficiency protects against focal cerebral ischemia

Laser Doppler flowmetry

To evaluate effects of TLR-4 deficiency on cerebral blood flow during and after MCA occlusion, LDF recordings were analyzed. In our studies, MCA occlusion resulted in a decrease of LDF values to ~15% of pre-ischemic levels (Figs. 1A and 2A). After reperfusion, LDF values normalized rapidly in animals subjected to 90 min MCA occlusion (Fig. 1A), but slightly increased above pre-ischemic values in animals submitted to 30 min ischemia (Fig. 2A). No differences were detected between wt and TLR-4 mutant (mt) mice.

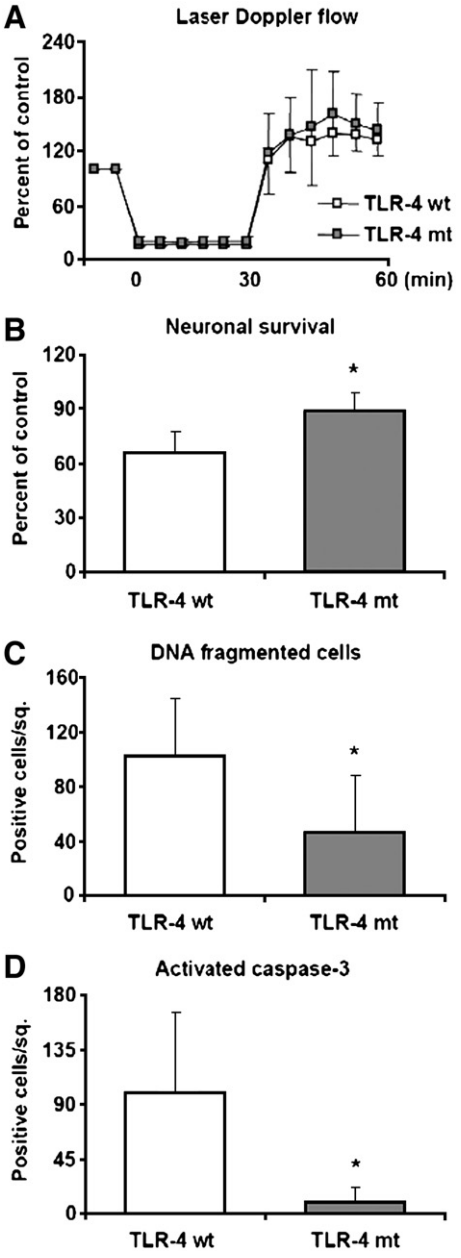

Fig. 2. Loss-of-function mutant TLR-4 promotes neuronal survival, decreases DNA fragmentation and reduces caspase-3 activation in the mouse striatum. LDF during and after ischemia (A), neuronal survival assessed by cresyl violet staining (B), DNA-fragmented cells evaluated by TUNEL (C), and activated caspase-3(+) cells (D) in TLR-4 wt and TLR-4 mt mice subjected to 30 min MCA occlusion, followed by 72 h reperfusion. Note again that LDF does not differ between mouse lines (A). Data are means±SD ($n=6$ animals/mouse line). *$p<0.05$ (two-tailed t-tests).

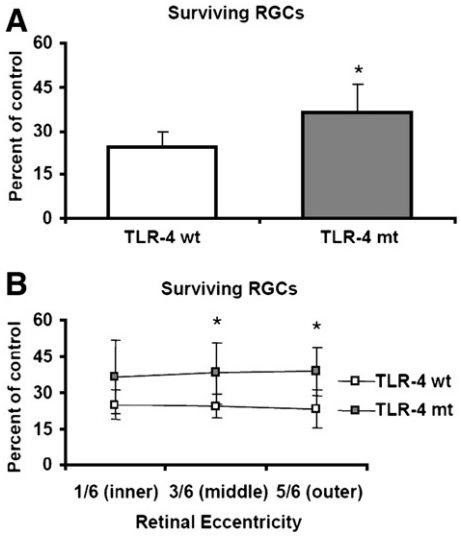

Fig. 3. TLR-4 deficiency protects axotomized RGCs from retrograde degeneration. Survival rates of fluorogold-prelabeled RGCs in TLR-4 wt and TLR-4 mt mice submitted to ON transsection, followed by 14 survivals. Survival rates averaged over the whole retina (A) and also survival rates at various retinal eccentricities (B) are shown. Data are means±SD ($n=6$ animals/mouse line). *$p<0.05$ (two-tailed t-tests).

Infarct volume and brain edema

As in previous studies (Kilic et al., 2006a; Bechmann et al., 2007), 90 min MCA occlusion resulted in focal infarcts of the cerebral cortex and underlying striatum in wt mice (Fig. 1B) that was reproducibly associated with brain edema (Fig. 1C). TLR-4 deficiency decreased infarct volume (Fig. 1B), without influencing brain swelling (Fig. 1C).

Selective neuronal injury and caspase-3 activation

As in earlier reports (Hermann et al., 2001; Wang et al., 2005), 30 min MCA occlusion induced selective neuronal injury in the striatum (Figs. 2B, C) that was accompanied by activation of caspase-3 (Fig. 2D). TLR-4 deficiency increased the percentage of surviving striatal neurons (Fig. 2B), reduced the density of DNA-fragmented, i.e., injured cells (Fig. 2C), and diminished caspase-3 activity (Fig. 2D).

TLR-4 mutation promotes the survival of axotomized RGCs

In non-lesioned retinae, RGC densities of TLR-4 mutant mice were slightly higher than those of wt animals (4115.7±263.2/mm^2 vs. 3321.1±508.8/mm^2, $p<0.05$), which may reflect an effect of TLR-4 on RGC survival during development. Upon ON transsection, reproducible RGC degeneration was noticed in retinae of wt mice, ~75% of RGCs undergoing delayed degeneration within 14 days (Figs. 3A, B). RGC damage was attenuated by TLR-4 deficiency (Figs. 3A, B).

TLR-4 deficiency reduces phosphorylation levels of ERK-1/-2, JNK-1/-2 and p38

To elucidate mechanisms underlying the neuroprotective effect of TLR-4 deficiency, Western blots were prepared using protein extracts obtained from brains subjected to focal cerebral ischemia. Western blots obtained with antibodies recognizing both unphosphorylated and phosphorylated MAP kinases revealed no differences in the overall expression of ERK-1/-2, JNK-1/-2 and p38 between wt and TLR-4 mt mice (Fig. 4). Phosphorylation levels of ERK-1/-2, JNK-1/-2 and p38, on the other hand, were markedly reduced by TLR-4 deficiency (Fig. 4).

TLR-4 deactivation downregulates neuronal iNOS expression

To evaluate how TLR-4 deficiency influences the expression of the pro-inflammatory protein iNOS, immunohistochemistries were evaluated. In animals submitted to 90 min, but not 30 min MCA occlusion, robust iNOS expression was noted in the ischemic brain parenchyma of wt mice that in the vast majority of cells (>80%) collocalized with the neuronal nuclear protein NeuN (Fig. 5A). TLR-4 deficiency downregulated neuronal iNOS levels in the ischemic brain tissue (Fig. 5A).

TLR-4 deficiency associated with compensatory PMN recruitment and microglial activation

To find out how TLR-4 deficiency influences the brain accumulation of blood-derived PMN as well as the activation of microglia — both cell types express TLR-4 on their cell surface (Lee and Kim, 2007), immunohistochemistries for MPO and Iba1 were prepared. Significant PMN recruitment and microglial reactivity was noted in ischemic brain areas in animals subjected to 90 min, but not 30 min MCA occlusion in wt mice (Figs. 5B, C). TLR-4 deficiency increased the density of MPO(+) PMN and of Iba1(+) ramified microglia in the ischemic tissue (Figs. 5B, C), most likely as compensatory mechanism counteracting the TLR-4 defect.

Discussion

We show that TLR-4 deficiency protects against rapidly developing ischemic and slowly progressive degenerative neuronal injury *in vivo* by mechanisms involving deactivation of ERK-1/-2, JNK-1/-2 and p38, downregulation of iNOS and inhibition of the executioner caspase-3. Our data were obtained using i.) the intraluminal MCA occlusion model, a highly reproducible and clinically relevant model of ischemic stroke, in which we evaluated two different durations of

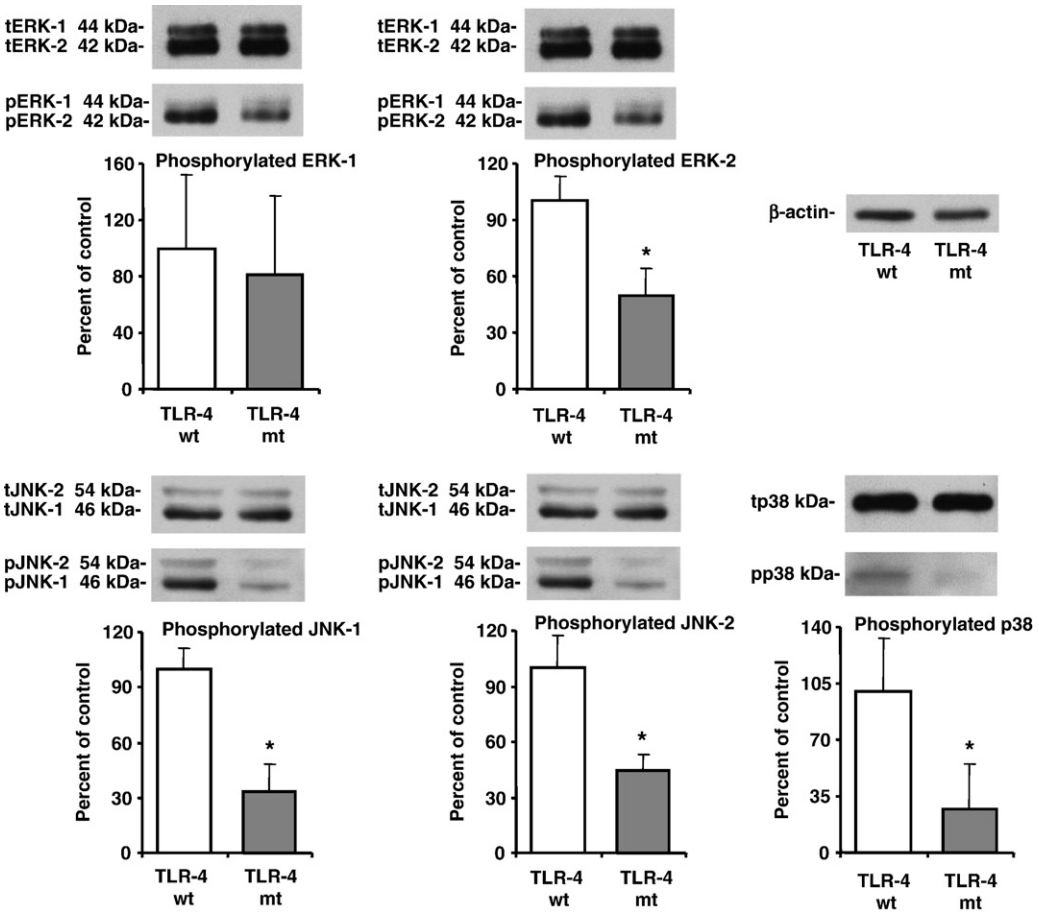

Fig. 4. Mutant TLR-4 decreases phosphorylated, but not total ERK-1/-2, JNK-1/-2 and p38. Western blots with protein extracts of tissue samples obtained from the ischemic cortex and underlying striatum of TLR-4 wt and TLR-4 mt mice submitted to 30 min MCA occlusion. Membranes were incubated with antibodies detecting both phosphorylated and non-phosphorylated (=total) protein kinases as well as antibodies that only recognize the phosphorylated, i.e., activated forms. Representative blots are also shown. Data are mean±S.D. ($n=3$ different blots/mouse line), normalized with corresponding blots for β-actin. *$p<0.05$ (two-tailed *t*-tests).

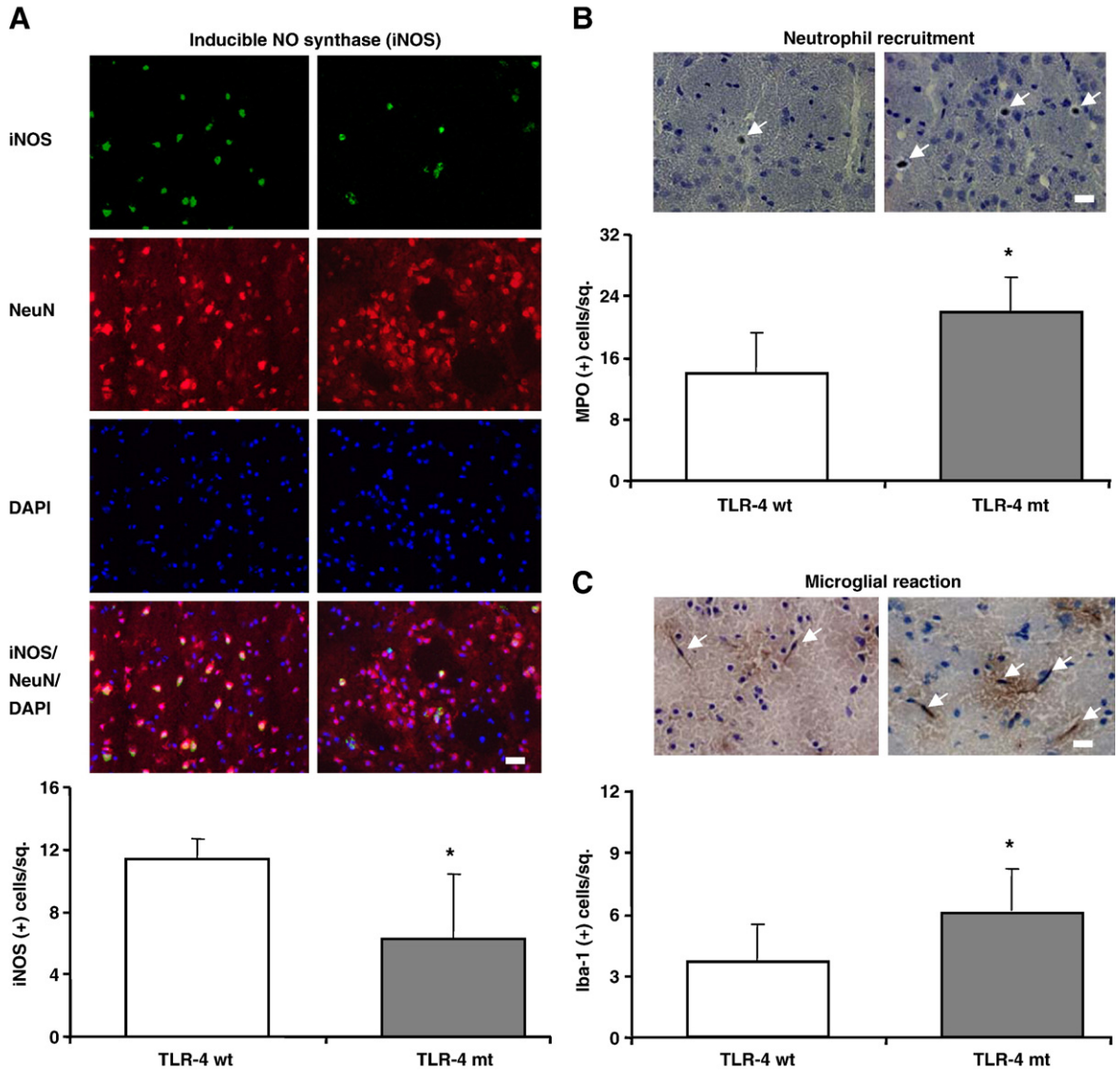

Fig. 5. TLR-4 deficiency downregulates inducible NO synthase (iNOS) in injured neurons, at the same time increasing polymorphonuclear neutrophil (PMN) recruitment and microglial activation in the stroke tissue. Density of iNOS + neurons (A), MPO(+) neutrophils (B) and Iba1(+) microglia (C) in TLR-4 wt and TLR-4 mt mice submitted to 90 min MCA occlusion, followed by 24 h reperfusion. Representative microphotographs exhibiting iNOS(+)/NeuN(+) neurons in the ischemic cortex are shown (A; counterstained with DAPI). Representative MPO(+) neutrophils and Iba1(+) microglia in the cortex are also depicted (B, C; counterstained with hematoxyline; labeled cells: see flashes). Data are means ± SD ($n = 6$ animals/mouse line). *$p < 0.05$ (two-tailed t-tests). Bar, 50 μm.

ischemia that result in reproducible brain infarcts (90 min MCA occlusion) (Hata et al., 2000; Kilic et al., 2006a) or selective neuronal injury (30 min ischemia) (Hermann et al., 2001; Wang et al., 2005;) and ii.) a model of RGC axotomy, in which the ON is cut close to the posterior eye pole (Isenmann et al., 1997; Klöcker et al., 1998; Kilic et al., 2006b). ON transsection leads to the degeneration of ~80% of RGCs within 14 days post-injury (Isenmann et al., 1997; Klöcker et al., 1998; Kilic et al., 2006b), thus mimicking more delayed neurodegenerative processes.

In our studies, we made use of the C3H/HeJ mouse line, which expresses a non-functional TLR-4 protein due to a point mutation in the receptor's cytosolic domain (Poltorak et al., 1998). While this paper was in the final stage of preparation, a manuscript from another group showed that *tlr*-4 deletion in C57bl/10ScNJ mice similar to loss-of-function mutant TLR-4 in C3H/HeJ animals reduces cortical injury following permanent MCA electrocoagulation (Caso et al., 2007). That *tlr*-4 knockout also promotes neuronal survival supports our present findings, providing additional evidence for TLR-4's harmful effects.

That TLR-4 deficiency protects against neuronal injury exemplifies the relationship between immune responses and neuronal degeneration, pointing out that signal responses triggered by PRR might set the pace for cell death programs (Zipp and Aktas, 2006). Our data suggest that TLR-4 might represent a promising target for neuroprotective therapies. TLR-4 is constitutively expressed in the CNS on microglia and macrophages (Lee and Kim, 2007), being involved in danger signaling to LPS, an outer cell wall constituent of gram-negative bacteria (Chakravarty and Herkenham, 2005).

By demonstrating that TLR-4 reduces ERK-1/-2, JNK-1/-2 and p38 phosphorylation, we provide insights into the mechanisms of neuroprotection induced by TLR-4 deficiency. In cultured macrophages, the LPS-induced release of tumor necrosis factor (TNF)-α was

previously shown to be mediated by MAP kinases (Schröder et al., 2001). Deactivation of TLR-4 using a monoclonal antibody abolished LPS-induced ERK-1/-2 phosphorylation, while pharmacological ERK-1/-2 and p38 blockade prevented LPS-induced TNF-α secretion (Schröder et al., 2001). By revealing that ERK-1/-2, JNK-1/-2 and p38, which are activated upon ischemia in wt mice (Kilic et al., 2005b), are dephosphorylated when TLR-4 is deactivated, we for the first time show that MAP kinases are involved in TLR-4 signaling *in vivo*.

Among the effectors contributing to immune-mediated injury in stroke and neurodegenerative diseases, iNOS is a well-established player (Dalkara and Moskowitz, 1994; Chan, 2001). Being induced in ischemic neurons (Kilic et al., 2006a) and axotomized RGCs (Klöcker et al., 1998), iNOS contributes to oxidative stress via formation of nitrite and nitrate (Dalkara and Moskowitz, 1994; Chan, 2001). By showing that TLR-4 deficiency downregulates iNOS in NeuN(+) ischemic neurons, we provide a link between immune surveillance, TLR-4-mediated cell signaling and neuronal injury pathways. Thus, a crosstalk exists between TLR-4(+) microglia and macrophages with brain neurons, which may explain TLR-4's neurodegeneration-promoting effects.

In contrast to neuronal iNOS that was reduced by TLR-4 deficiency, the recruitment of blood-derived PMN and activation of microglia was increased in ischemic tissue of our C3H/HeJ mouse line. PMN leucocytes similar to brain-resident microglia and macrophages express TLR-4 on their cell surface (Lee and Kim, 2007). That PMN accumulation and microglial activation were increased in the brains of ischemic TLR-4 mt animals might represent a futile, compensatory mechanism, aiming to counterbalance consequences of the gene defect. Apparently, the increased PMN and microglia recruitment did not exert any injurious effect, pointing out that PMN invasion and microglial activation are not necessarily detrimental to the brain.

The enhanced neuronal survival in TLR-4 deficient mice raises the question whether deactivation strategies of innate immune receptors may be used for clinical purposes in the future. Our here-presented data support this fascinating idea. Yet, when evaluating strategies of PRR blockade, long-term effects of receptor deactivation for immune function should carefully be considered. Rodent studies have shown that stroke represents a particularly vulnerable immunodepressant state in which bacterial infection may occur more easily than normal (Prass et al., 2006). Thus, care must be taken that survival-promoting effects are not achieved at the expense of infectious states. Further studies should further elucidate the therapeutic potential of strategies modulating PRR signaling in ischemic stroke and neurodegenerative diseases. Such studies may help to clarify whether innate immunity is indeed a promising target for neuroprotection therapies.

Acknowledgments

This research was supported by the Swiss National Center of Competence (NCCR) 'Neural plasticity', the Center for Integrative Human Physiology (CIHP), the Swiss National Science (3200B0-112056/1), the Baasch-Medicus, Hermann-Klaus, David-and-Betty-Koetser and Hartmann-Müller Foundation (all to D.M.H.).

References

Bechmann, I., Galea, I., Perry, V.H., 2007. What is the blood-brain barrier (not)? Trends Immunol. 28, 5–11.

Begley, D.J., 2004. Delivery of therapeutic agents to the central nervous system: the problems and the possibilities. Pharmacol. Ther. 104, 29–45.

Bermpohl, D., Halle, A., Freyer, D., Dagand, E., Braun, J.S., Bechmann, I., Schröder, N.W., Weber, J.R., 2005. Bacterial programmed cell death of cerebral endothelial cells involves dual death pathways. J. Clin. Invest. 115, 1607–1615.

Caso, J.R., Pradillo, J.M., Hurtado, O., Lorenzo, P., Moro, M.A., Lizasoain, I., 2007. Toll-like receptor-4 is involved in brain damage and inflammation after experimental stroke. Circulation 115, 1599–1608.

Chakravarty, S., Herkenham, M., 2005. Toll-like receptor 4 on nonhematopoietic cells sustains CNS inflammation during endotoxemia, independent of systemic cytokines. J. Neurosci. 25, 1788–1796.

Chan, P.H., 2001. Reactive oxygen radicals in signaling and damage in the ischemic brain. J. Cereb. Blood Flow Metab. 21, 2–14.

Dalkara, T., Moskowitz, M.A., 1994. The complex role of nitric oxide in the pathophysiology of focal cerebral ischemia. Brain Pathol. 4, 49–57.

Hata, R., Maeda, K., Hermann, D.M., Mies, G., Hossmann, K.A., 2000. Dynamics of regional brain metabolism and gene expression after middle cerebral artery occlusion in mice. J. Cereb. Blood Flow Metab. 20, 306–315.

Hermann, D.M., Bassetti, C.L., 2007. Implications of ATP-binding cassette transporters for brain pharmacotherapies. Trends Pharmacol. Sci. 28, 128–134.

Hermann, D.M., Kilic, E., Hata, R., Hossmann, K.A., Mies, G., 2001. Relationship between metabolic changes, gene responses and delayed ischemic injury after mild focal cerebral ischemia in mice. Neuroscience 104, 947–955.

Hermann, D.M., Kilic, E., Spudich, A., Krämer, S.D., Wunderli-Allenspach, H., Bassetti, C.L., 2006. Role of drug efflux carriers in the healthy and diseased brain. Ann. Neurol. 60, 489–498.

Isenmann, S., Wahl, C., Krajewski, S., Reed, J.C., Bähr, M., 1997. Up-regulation of Bax protein in degenerating retinal ganglion cells precedes apoptotic cell death after optic nerve lesion in the rat. Eur. J. Neurosci. 9, 1763–1772.

Kilic, Ü., Kilic, E., Soliz, J., Bassetti, C.L., Gassmann, M., Hermann, D.M., 2005a. Erythropoietin protects from axotomy-induced degeneration of retinal ganglion cells by activating ERK-1/-2. FASEB J. 19, 249–251.

Kilic, Ü., Kilic, E., Xing, H., Wang, Z., Bassetti, C.L., Hermann, D.M., 2005b. Post-ischemic delivery of the 3-hydroxy-3-methylglutaryl coenzyme A reductase inhibitor rosuvastatin protects against focal cerebral ischemia in mice by mechanisms involving inhibition of extracellular-regulated kinase-1/-2. Neuroscience 106, 901–906.

Kilic, E., Kilic, Ü., Wang, Y., Bassetti, C.L., Marti, H.H., Hermann, D.M., 2006a. The phosphatidylinositol-3 kinase/Akt pathway mediates VEGF's neuroprotective activity and induces blood brain barrier permeability after focal cerebral ischemia. FASEB J. 20, 1185–1187.

Kilic, Ü., Kilic, E., Järve, A., Guo, Z., Spudich, A., Bieber, K., Barzena, U., Bassetti, C.L., Marti, H.H., Hermann, D.M., 2006b. Human vascular endothelial growth factor protects axotomized retinal ganglion cells in vivo by activating ERK-1/2 and Akt pathways. J. Neurosci. 26, 12439–12446.

Klöcker, N., Cellerino, A., Bähr, M., 1998. Free radical scavenging and inhibition of nitric oxide synthase potentiates the neurotrophic effects of BDNF on axotomized retinal ganglion cells in vivo. J. Neurosci. 18, 1038–1046.

Lee, M.S., Kim, Y.J., 2007. Signaling pathways downstream of pattern-recognition receptors and their cross talk. Annu. Rev. Biochem. 76, 447–480.

Lemaitre, B., Nicolas, E., Michaut, L., Reichhart, J.M., Hoffmann, J.A., 1996. The dorsoventral regulatory gene cassette spatzle/Toll/cactus controls the potent antifungal response in *Drosophila* adults. Cell 86, 973–983.

Löscher, W., Potschka, H., 2005. Drug resistance in brain diseases and the role of drug efflux transporters. Nat. Rev., Neurosci. 6, 591–602.

Poltorak, A., He, X., Smirnova, I., Liu, M.H., van Huffel, C., Du, X., Birdwell, D., Alejos, E., Silva, M., Galanos, C., Freudenberg, M., Ricciardi-Castagnoli, P., Layton, B., Beutler, B., 1998. Detective LPS signaling in C3H/HeJ and C57BL/10ScCr mice: mutations in TLR4 gene. Science 282, 2085–2088.

Prass, K., Braun, J.S., Dirnagl, U., Meisel, C., Meisel, A., 2006. Stroke propagates bacterial aspiration to pneumonia in a model of cerebral ischemia. Stroke 37, 2607–2612.

Sansonetti, P.J., 2006. The innate signaling of dangers and the dangers of innate signalling. Nat. Immunol. 7, 1237–1242.

Spudich, A., Kilic, E., Xing, H., Kilic, Ü., Rentsch, K.M., Wunderli-Allenspach, H., Bassetti, C.L., Hermann, D.M., 2006. Inhibition of multidrug resistance transporter-1 facilitates neuroprotective therapies after focal cerebral ischemia. Nat. Neurosci. 9, 487–488.

Sutmuller, R.P.M., Morgan, M.E., Netea, M.G., Grauer, O., Adema, G.J., 2006. Toll-like receptors on regulatory T cells: expanding immune regulation. Trends Immunol. 27, 387–393.

Schröder, N.W., Pfeil, D., Opitz, B., Michelsen, K.S., Amberger, J., Zahringer, U., Gobel, U.B., Schumann, R.R., 2001. Activation of mitogen-activated protein kinases p42/44, p38, and stress-activated protein kinases in myelo-monocytic cells by Treponema lipoteichoic acid. J. Biol. Chem. 276, 9713–9719.

Wang, Y., Kilic, E., Kilic, Ü., Weber, B., Bassetti, C.L., Marti, H.H., Hermann, D.M., 2005. VEGF overexpression induces post-ischaemic neuroprotection, but facilitates haemodynamic steal phenomena. Brain 128, 52–63.

Zipp, F., Aktas, O., 2006. The brain as a target of inflammation: common pathways link inflammatory and neurodegenerative diseases. Trends Neurosci. 29, 518–527.